35th Annual International Conference of the IEEE EMBS
Osaka, Japan, 3 - 7 July, 2013

Characteristics of magnetic probes for identifying sentinel lymph nodes

Tetsu Ookubo, Yusuke Inoue, Dongmin Kim, Hiroyuki Ohsaki, *Member*, *IEEE*, Yusuke Mashiko, Moriaki Kusakabe, and Masaki Sekino ,*Member, IEEE*

***Abstract*— The identification of the sentinel lymph nodes that cause tumor metastasis is important in breast cancer therapy. The detection of magnetic fluid accumulating in the lymph nodes using a magnetic probe allows surgeons to identify the lymph nodes. In this study, we carried out numerical simulations and experiments to investigate the sensitivity and basic characteristics of a magnetic probe consisting of a permanent magnet and a small magnetic sensor. The measured magnetic flux density arising from the magnetic fluid agreed well with the numerical results. In addition, the results helped realize an appropriate probe configuration for achieving high sensitivity to magnetic fluid. A prototype probe detected magnetic fluid located 30 mm from the probe head.**

I. INTRODUCTION

The sentinel lymph node refers to the lymph node to which cancer cells first reach from a cancerous lesion through the lymphatic vessels. In breast cancer treatment, the occurrence of metastases is investigated by conducting a sentinel lymph node biopsy, the results of which provide a basis for selecting an appropriate treatment. Sentinel lymph node biopsy is an essential step in breast cancer treatment and is currently carried out using a radioisotope [1, 2] or a dye [3] as the source of tracer particles. However, these methods have some problems. Few hospitals have the equipment required for using radioisotopes, and the use of radioactive tracers exposes not only patients but also medical staff to radiation. Moreover, it is difficult to identify the sentinel lymph node correctly using coloring matter. Other sentinel lymph node biopsy methods include one involving the use of a superconducting quantum interference device (SQUID) [4, 5] and one using the nonlinear response of magnetic particles [6−8]. However, the SQUID-sensor-based method requires refrigerant and associated infrastructure.

We aim to develop a method for identifying the sentinel lymph nodes by injecting magnetic fluid into the breast and using a magnetic probe for detecting the injected magnetic fluid. Figure 1 illustrates the operation of the magnetic probe. Magnetic fluid injected into the breast flows into the sentinel lymph nodes, and it is detected by the magnetic probe. This magnetic probe has a simple structure consisting of a permanent magnet and magnetic sensor, thus allowing immediate clinical application.

In the present study, we carried out a numerical simulation and fabricated a prototype magnetic probe. Basic characteristics of the magnetic probe were evaluated experimentally. We showed it can be used for identifying the sentinel lymph nodes that may be located at distances of up to 30 mm from the probe head.

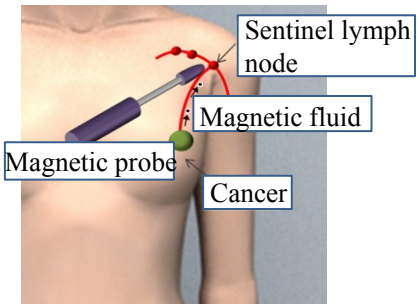

Figure 1. Sentinel lymph nodes identification using magnetic probe

II. PROBE DESIGN

Figures 2 and 3 show the schematic structure and a photograph of the prototype, respectively, of the developed magnetic probe.

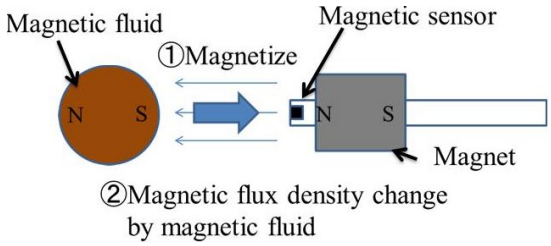

Figure 2. Structure of the proposed magnetic probe

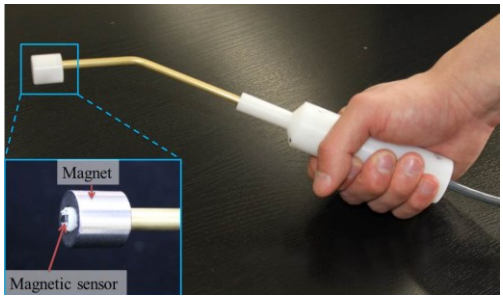

Figure 3. Prototype of developed magnetic probe

T. Ookubo is with Department of Electrical and Electronic Engineering, Faculty of Engineering, The University of Tokyo, Tokyo 113-8656, Japan (e-mail: ookubo@bee.t.u-tokyo.ac.jp)

Y. Inoue, D. Kim and M. Sekino are with Department of Electrical Engineering and Information Systems, Graduate School of Engineering, The University of Tokyo, Tokyo 113-8656, Japan, and also with Exploratory Research for Advanced Technology, Japan Science and Technology Agency, Tokyo 113-8656, Japan (e-mail: inoue@bee.t.u-tokyo.ac.jp; dongmin@bee.t.u-tokyo.ac.jp; sekino@bee.t.u-tokyo.ac.jp)

H. Ohsaki is with Department of Advanced Energy, Graduate School of Frontier Sciences, The University of Tokyo, Chiba 277-8561, Japan (e-mail: ohsaki@k.u-tokyo.ac.jp)

Y. Mashiko is with Kyoshin Co., Ltd, Tochigi 325-0033, Japan (e-mail: mashiko@ksn-g.co.jp)

M. Kusakabe is with Research Center for Food Safety, Graduate School of Agricultural and Life Science, The University of Tokyo, Tokyo 113-8657, Japan (e-mail: amkusa@mail.ecc.u-tokyo.ac.jp)

The prototype magnetic probe was designed for use in a common operating room. The magnetic probe consists of a ring-shaped permanent magnet, small magnetic sensor, and nonmagnetic shaft. When a magnetic fluid approaches the magnetic probe, the coercivity of the permanent magnet induces a magnetization of the fluid. Consequently, the magnetic flux density applied to the small magnetic sensor varies. The magnetic probe identifies the presence of the magnetic fluid by detecting this variation. Because the magnetic fluid has to be safe for use with the human body, we use Resovist, a contrast-enhanced agent commonly used in magnetic resonance imaging. In this study, a Hall-effect sensor, giant magnetoresistance (GMR) sensor, and magnetoimpedance (MI) sensor were used as the small magnetic sensors. These sensors detect magnetic flux density. The detectable range of Hall-effect sensor and GMR sensor are from $10^{0}$to 10^{-6} and that of MI sensor is from 10^{-2} to 10^{-10}.

III. Numerical Simulations

Numerical simulations were carried out to investigate the change in magnetic field distributions due to the magnetic fluid.

Figure 4 shows the lines of magnetic flux around the sensor and shows the point at which magnetic flux density is zero. On the central axis, there are two points where magnetic flux density is zero. The small magnetic sensor is placed at this point. This sensor placement allows for increased amplification, thus ensuring that the magnetic probe detects small changes in magnetic flux density. Of these two points, the one that is closer to the top of the permanent magnet is the reference point for defining the distance of magnetic fluid. The value of magnetic flux density at this point with no magnetic fluid is A. The value of magnetic flux density at this point considering magnetic fluid placed at a fixed point is B. Furthermore $\Delta B = B - A$ where ΔB is the sensitivity. Higher the ΔB value, greater is the flux density change induced by the magnetic fluid.

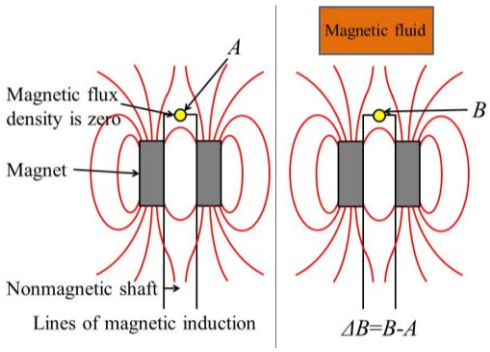

Figure 4. Magnetic induction lines around sensor

In this study, we used the finite-element method to analyze electromagnetic fields. Figure 5 (a) shows the numerical simulation model of the probe and magnetic fluid. This magnetic probe consisted of a nonmagnetic shaft at the center and a permanent magnet on the outside. The relative permeability of the nonmagnetic shaft was 1.0, which was the same as that of air. In the numerical simulation, we varied the distance between the reference point and magnetic flux density as 10, 20, and 30 mm. The numerical simulation model was of the axial symmetry type. The relative permeability of the permanent magnet was 1.05, and its coercivity was 976 kA/m. The magnetic fluid was contained in a column whose radius was 10 mm and height was 5.1 mm. The characteristic of the magnetic fluid was given by a B-H curve data measured using a SQUID system. Figure 5 (b) shows the finite elements of this model. The finite elements around the permanent magnet and magnetic fluid were relatively small.

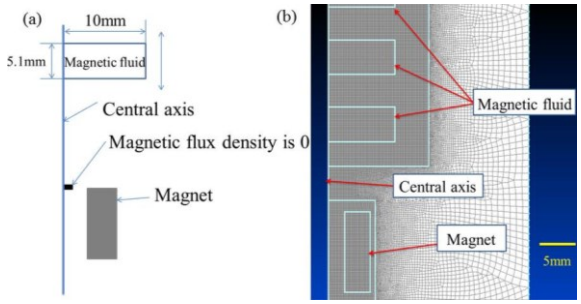

Figure 5. Numerical model of magnetic probe ((a) numerical model and (b) finite elements)

Figure 6 shows the contour map of magnetic flux density around the magnetic probe and magnetic fluid, obtained from the numerical simulation. The results show that the field distribution slightly changes when the distance between the magnetic fluid and the sensor is 10 mm or 20 mm, but there is almost no change when the distance is 30 mm. Figure 7 shows the dependence of magnetic flux density on sensor position. Changes of magnetic flux density became greater when the reference point was closer to the magnetic fluid.

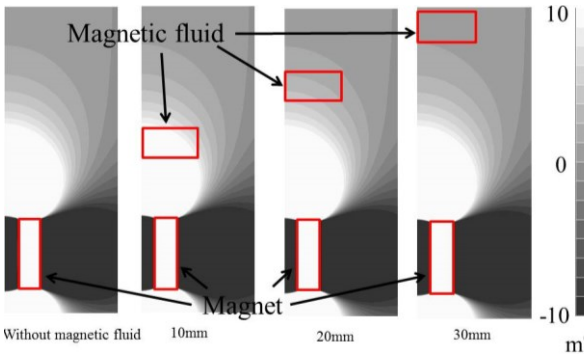

Figure 6. Contour maps of magnetic flux density around magnetic probe and magnetic fluid

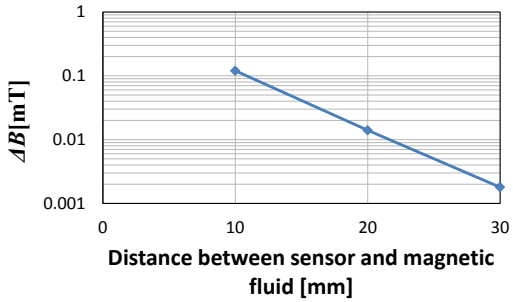

Figure 7. Intensity of magnetic fields applied to sensor

IV. Experiments for Detecting Magnetic Fluid

We developed an experimental setup for determining the most appropriate type of small magnetic sensor. This experiment is not in vivo experiment nor in vitro one. The best position of the permanent magnet relative to the sensor was determined experimentally and compared with the results of the numerical simulation. We obtained experimental data using three types of magnetic sensors; Hall-effect sensor, GMR sensor, and MI sensor.

The experimental process was as follows.

(1) The output from each sensor was measured at various distances between the sensor and permanent magnet. We found the distance where the output magnetic flux density was zero.

(2) The permanent magnet was fixed at the point where the sensor indicated zero magnetic flux density. Thereafter, the distance between the small magnetic sensor and the magnetic fluid was varied, and the output from each sensor was measured.

(3) When the position of the permanent magnet was changed, the change in the output of each sensor was measured in both the presence and absence of the magnetic fluid.

Figure 8 schematically shows the detection experiments. The sensor output was amplified and recorded using an oscilloscope.

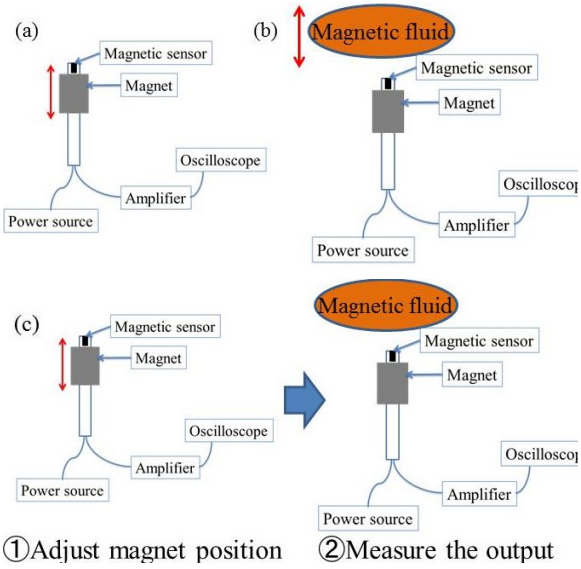

Figure 8. Experimental setup for detecting magnetic fluid ((a) Changing distance between permanent magnet and magnetic sensor. (b) Changing distance between magnetic fluid and magnetic sensor. (c) Changing distance while introducting magnetic fluid near the probe.)

Following are the results of the detection experiments.

(1) Hall-effect sensor

The distance between the sensor and the permanent magnet was changed with sensor currents of 5, 10 and 15 mA. Figure 9 shows the magnetic flux density at the sensor's location. For sensor currents of 5, 10, and 15 mA, the distances between the sensor and the top of the magnet were 0.93, 0.97, and 0.93 mm, respectively.

The magnet was fixed at the point where the measured magnetic flux density was zero. Then, the distance between the small magnetic sensor and the magnetic fluid was varied. Figure 10 shows the variations in magnetic flux density at this sensor position. The experimental results agree well with those of numerical simulation given in Fig. 7.

Figure 11 shows the changes in sensor output caused by the presence of magnetic fluid at each magnet position. The position of the permanent magnet was changed. Comparing Fig. 9 and Fig. 11, when the magnet was fixed at the point where the magnetic flux density was zero, the sensitivity of the magnetic probe was the highest.

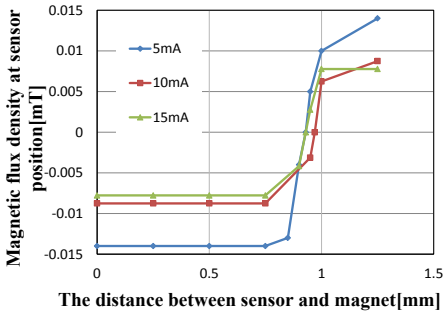

Figure 9. Dependence of measured magnetic flux density on distance between the permanent magnet and Hall-effect sensor

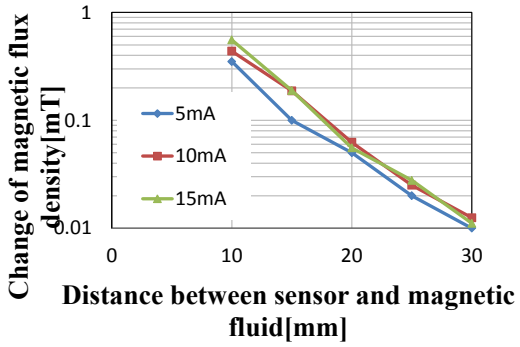

Figure 10. Dependence of magnetic flux density on distance between magnetic fluid and Hall-effect sensor

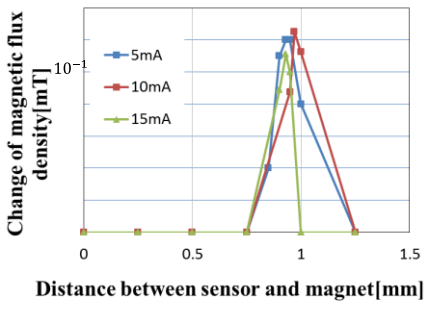

Figur 11. Variation in magnetic flux density owing to existence of magnetic fluid while changing distance between permanent magnet and Hall-effect sensor

(2) GMR sensor

The input voltage was 20 V. Figure 12 shows the magnetic flux density at the small magnetic sensor's location when the distance between it and the top of the permanent magnet was varied. The point where the magnetic flux density was zero was about 0.6 mm.

The permanent magnet was fixed at the point where the magnetic flux density was zero. The distance between the small magnetic sensor and the magnetic fluid was varied, and the sensor output was measured. However, the change in magnetic flux density could not be measured when the distance between the sensor and the fluid was greater than 5 mm.

Figure 13 shows variation in the sensor output caused by the magnetic fluid at each magnet position. Comparing Fig. 12 and Fig. 13, when the magnet was fixed at a position where the magnetic flux density was zero, the sensitivity of the magnetic probe was at its highest.

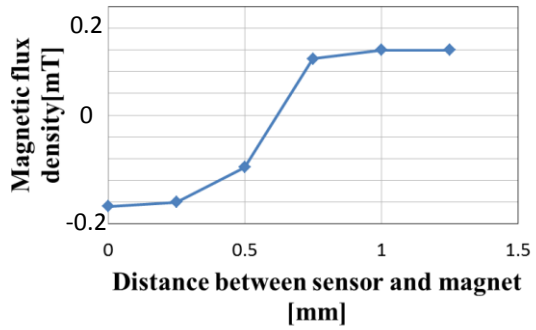

Figure 12. Change in magnetic flux density as a function of distance between permanent magnet and GMR sensor

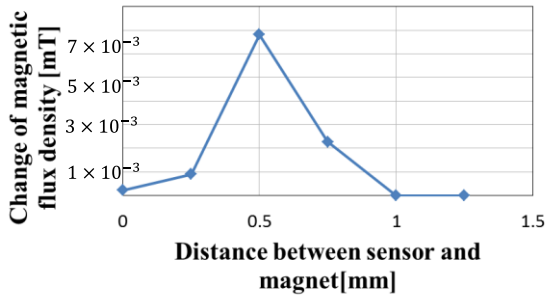

Figure 13. Dependence of magnetic flux density on distance between permanent magnet and GMR sensor

(3) MI sensor

When the MI sensor was located near the permanent magnet, the output voltage was fully saturated.

V. Discussion

The GMR and MI sensors could not detect the magnetic fluid to the desired extent. This is attributed to magnetic field heterogeneity around the point where the magnetic flux density was zero. The gradient of magnetic flux density at the sensor position was very steep. The magnetic flux density was largely heterogeneous even within the sensor's active area.

When the Hall-effect sensor was used as the small magnetic sensor, a change in the magnetic flux density with the distance between the magnetic fluid and the small magnetic sensor was recorded, as is shown in Fig. 10. The result shows that magnetic flux density at the sensor position was about 10 μT when the distance between the magnetic fluid and the small magnetic sensor was 30 mm. This means that a magnetic probe equipped with a Hall-effect sensor can detect 1.6 mL of magnetic fluid at a distance of 30 mm. However, the volume of magnetic fluid reaching the sentinel lymph node is less than 1.6 mL. Therefore it is required that the probe's sensitivity to a smaller volume of magnetic fluid be investigated.

VI. Conclusions

We carried out numerical simulations and experiments to investigate the basic characteristics of the proposed magnetic probe. Three small magnetic sensors were compared in terms of their sensitivity to magnetic fluid. The experimentally measured magnetic flux density owing to the magnetic fluid agreed well with the numerically determined values. The position of magnetic sensor at which the probe exhibited maximum sensitivity corresponded to the location where the magnetic flux density was zero in the absence of magnetic fluid. The Hall-effect sensor was the most sensitive and stable from the viewpoint of use in magnetic probes.

References

[1] R. J. de Hass, D. A. Wicherts, M. G. G. Hobbelink, P. J. van Diest, F. P. Vleggaar, I. H. M. Borel-Rinkes, and R. van Hillegersberg, "Sentinel lymph node mapping in colon cancer using radiocolloid as a single tracer: a feasibility study," *Nucl. Med. Commun.*, vol. 33, no.8, pp. 832-837, 2012.

[2] J. S. Radowsky, L. Baines, R. S. Howard, C. D. Shriver, C. C. Buckenmaier III , and A. Stojadinovic, "Pain ratings by patients and their providers of radionucleotide injection for breast cancer lymphatic mapping," *Pain Medicine,* vol.13, no.5, pp.670-676, 2012

[3] K. Aoyama, T. Kamoi, T. Ohchi, M. Nishizawa, and S. Kameoka, " Sentinel lymph node biopsy for breast cancer patients using fluorescence navigation with indocyanine green," *World J. Surg. Oncol.*, vol.9, pp.157, 2011

[4] S. Tanaka, A. Hirata, Y. Saito, T. Mizoguchi, Y. Tamaki, I. Sakita and M. Monden," Application of high Tc SQUID magnetometer for sentinel-lymph node biopsy," *IEEE Trans. Appl. Supercond.*, vol.11, no.1, pp.665-668, 2001

[5] S. Tanaka, H. Ota, Y. Kondo, Y. Tamaki, S. Kobayashi, and S. Noguchi," Detection of magnetic nanoparticles in lymph nodes of rat by high Tc SQUID," *IEEE Trans. Appl. Supercond.*, vol.13, no.2, pp.377-380, 2003

[6] B. Gleich and J. Weizenecker," Tomographic imaging using the nonlinear response of magnetic particles," *Nature*, vol 435, pp.1214-1217, 2005

[7] J.J. Chieh, H.E. Horng, W.K. Tseng, S.Y. Yang, C.Y. Horng, H.C. Yang, and C.C. Wu, "Imaging the distribution of magnetic nanoparticles on animal bodies using scanning SQUID biosusceptometry attached with avideo camera," *IEEE Trans. Apple. Supercond.*, vol.23, no.3, p.1601503, 2013

[8] W. K. Tseng, J. J. Chieh, Y. F. Yang, C.K. Chiang, Y.L. Chen, S. Y. Yang, H. E. Horng, H. C. Yang, and C. C. Wu, "A noninvasive method to determine the fate of Fe_3O_4 nanoparticle following intravenous injection using scanning SQUID biosusceptometry" *PLoS One*, vol.7,issue11, e48510, 2012